

NACA-TN-1345

# NATIONAL ADVISORY COMMITTEE FOR AERONAUTICS

TECHNICAL NOTE

No. 1345

CRITICAL COMBINATIONS OF TORSION AND DIRECT  
AXIAL STRESS FOR THIN-WALLED CYLINDERS

By S. B. Batdorf, Manuel Stein, and Murry Schildcrout

Langley Memorial Aeronautical Laboratory  
Langley Field, Va.



Washington  
June 1947

REPRODUCED BY  
NATIONAL TECHNICAL  
INFORMATION SERVICE  
U.S. DEPARTMENT OF COMMERCE  
SPRINGFIELD, VA. 22161



NATIONAL ADVISORY COMMITTEE FOR AERONAUTICS

TECHNICAL NOTE NO. 1345

CRITICAL COMBINATIONS OF TORSION AND DIRECT  
AXIAL STRESS FOR THIN-WALLED CYLINDERS

By S. B. Batdorf, Manuel Stein, and Murry Schilderout

SUMMARY

A theoretical solution is presented for the determination of the combinations of direct axial stress and torsion which cause thin-walled cylinders with either simply supported or clamped edges to buckle. This theoretical solution is used in conjunction with available test data to develop empirical curves and formulas for use in design. Comparisons are made with theoretical and empirical solutions obtained in other investigations.

INTRODUCTION

The determination of the combinations of direct axial stress and torsion which cause thin-walled cylinders to buckle is treated in the present paper. Cylinders in torsion buckle at a stress slightly less than the theoretical stress (reference 1) and cylinders in compression buckle at a stress considerably less than the theoretical stress (reference 2). It therefore appears that the theoretical solution would be in good agreement with the experimental results when the buckling is due mainly to torsion but would require modifications when the buckling is to any appreciable extent due to compression.

Empirical approaches to the problem have been made previously (references 3 to 5) and interaction formulas have been proposed for use in design. These formulas are somewhat limited as to the range of applicability because of the limited range of dimensions of the test specimens.

In the present paper theoretical interaction curves are derived (appendix A), the test data of references 3 to 5 are re-examined, and finally empirical interaction curves and formulas that are rational modifications of the theory are developed. The present results can therefore be used over a much wider range of cylinder

dimensions than could previously available results. In the analysis given herein the theoretical results are first described and then modifications are introduced to bring the results into agreement with available experimental data.

## SYMBOLS

$m, n, j$	integers
$r$	radius of cylinder
$t$	thickness of cylinder wall
$u$	displacement of point on median surface of cylinder in axial (x-) direction
$v$	displacement of point on median surface of cylinder in circumferential (y-) direction
$w$	displacement of point on median surface of cylinder in radial direction; positive outward
$x$	axial coordinate of cylinder
$y$	circumferential coordinate of cylinder
$D$	flexural stiffness of plate per unit length $\left( \frac{Et^3}{12(1-\mu^2)} \right)$
$E$	Young's modulus of elasticity
$L$	length of cylinder
$Q$	operator defined in appendix A
$Z$	curvature parameter $\left( \frac{L^2}{rt} \sqrt{1-\mu^2} \right)$ or $\left( \frac{L}{r} \right)^2 \frac{r}{t} \sqrt{1-\mu^2}$
$a_n, b_n$	coefficients of terms in deflection functions
$k_s$	shear-stress coefficient appearing in equation $\tau = \frac{k_s \pi^2 D}{L^2 t}$

$k_x$  direct-axial-stress coefficient appearing in  
equation  $\sigma_x = \frac{k_x \pi^2 D}{L^2 t}$

$$M_n = \frac{\pi}{8\beta} \left[ (n^2 + \beta^2)^2 + \frac{12Z^2 n^4}{\pi^4 (n^2 + \beta^2)^2} - n^2 k_x \right]$$

$(R_s)_{\text{exp}}$  empirical shear-stress ratio (ratio of shear stress present to empirical critical shear stress in absence of other stresses)

$(R_s)_{\text{th}}$  theoretical shear-stress ratio (ratio of shear stress present to theoretical critical shear stress in absence of other stresses)

$(R_x)_{\text{exp}}$  empirical direct-axial-stress ratio (ratio of direct axial stress present to empirical critical direct axial stress in absence of other stresses)

$(R_x)_{\text{th}}$  theoretical direct-axial-stress ratio (ratio of direct axial stress present to theoretical critical direct stress in absence of other stresses)

$V_m, W_m$  deflection functions defined in appendix A

$$\beta = \frac{L}{\lambda}$$

$\lambda$  half wave length of buckles in circumferential direction

$\mu$  Poisson's ratio

$\sigma_x$  direct axial stress in cylinder wall

$\tau$  shear stress in cylinder wall

$$\nabla^4 = \frac{\partial^4}{\partial x^4} + 2 \frac{\partial^4}{\partial x^2 \partial y^2} + \frac{\partial^4}{\partial y^4}$$

$\nabla^{-4}$  = inverse of  $\nabla^4$ , defined by  $\nabla^{-4} \nabla^4 w = w$

## RESULTS AND DISCUSSION

Theoretical interaction curves.- The combinations of shear and axial stress which cause cylinders to buckle may be obtained from the equations

$$\tau = \frac{k_s \pi^2 D}{L^2 t}$$

and

$$\sigma_x = \frac{k_x \pi^2 D}{L^2 t}$$

when the stress coefficients  $k_s$  and  $k_x$  are known. The theoretical combinations of shear-stress and axial-stress coefficients for cylinders with simply supported or clamped edges are given by interaction curves for a number of values of the curvature parameter  $Z$  in figures 1(a) and 1(b), respectively.

For small values of  $Z$ , which describe very short cylinders, the interaction curves have vertical parts which are discussed in some detail in reference 6 and in appendix B of the present paper. At slightly larger values of  $Z$  the curves have the general shape of a parabola and at still larger values of  $Z$  the curves tend to straighten out. Computations show that curves plotted in stress-ratio form for simply supported cylinders are substantially independent of the value of  $Z$  from  $Z = 30$  to at least  $Z = 1000$ , the largest value of  $Z$  that was checked. Such interaction curves were not computed for cylinders with clamped edges at large values of  $Z$ ; however, at large values of  $Z$ , the critical stresses in both shear alone and in compression alone are substantially independent of the type of edge support. The interaction curve therefore can reasonably be assumed to be almost independent of the type of edge support. The interaction curves for cylinders having values of  $Z$  greater than 30 with either simply supported or clamped edges may be approximated in the compression range by a straight line from  $(R_x)_{th} = 1$  to  $(R_s)_{th} = 1$  and early in the tension range by a straight line having a slope of  $-0.8$  passing through  $(R_s)_{th} = 1$  (see fig. 2). The denominators of the stress ratios  $(R_s)_{th}$  and  $(R_x)_{th}$  are the critical stresses for torsion

alone and for axial compression alone, which may be obtained from the theoretical curves of figures 3 and 4, taken from references 1 and 2, respectively. The theoretical interaction data that have been computed are given in table 1.

Very long cylinders in torsion ( $Z > \text{about } 10\frac{r^2}{t^2}$ ) buckle with two circumferential half waves and the curves of figure 3 no longer apply (see reference 1). The curves of figure 4, which describe the local instability of cylinders, do not apply to very long cylinders which fail as Euler columns (Euler buckling occurs for  $Z > \text{about } 7.7\frac{r^2}{t^2}$  for simply supported cylindrical columns). The present paper is solely concerned with short and moderately long cylinders - say,  $Z < 7.7\frac{r^2}{t^2}$ .

Empirical interaction curves.- As cylinders of moderate or large curvature buckle in compression at a stress considerably less than the theoretical stress, the curves in figures 1(a) and 1(b) and the interaction data of table 1 must be modified to give results applicable to actual cylinders. The requirement that for large values of  $Z$  the empirical interaction curve should agree approximately with the theoretical curve near the  $k_s$ -axis and yet cross the  $k_x$ -axis at only a fraction of the theoretical  $k_x$ -intercept suggests the use of a curve of the parabolic type in the compression range. Available experimental data indicate that the analysis required to determine the type of parabola most satisfactory from a theoretical point of view for each particular cylinder is not justified for practical purposes because of the scatter of the test points and that the use of the simple parabola  $(R_s)_{\text{exp}}^2 + (R_x)_{\text{exp}} = 1$  is satisfactory.

The simple parabolic interaction curve is completely determined when the intercepts corresponding to pure torsion and pure compression are known. These intercepts may be obtained from the empirical curves of figures 3 and 4. The empirical curves for cylinders under compression were obtained from reference 2, and the empirical curves for cylinders under torsion were obtained by fairing a curve through the test points given in reference 1.

References 1 and 2 indicate that theory and experiment are in good agreement for either torsion or compression alone for very short cylinders ( $Z \leq 1$  for simply supported edges and  $Z \leq 5$  for clamped edges). In these ranges of  $Z$ , therefore, the theoretical

interaction curves (figs. 1(a) and 1(b)) and values from table 1 may be used. At larger values of  $Z$  parabolic interaction curves with intercepts obtained from the empirical curves of figures 3 and 4 are recommended for use in the compression range.

In the tension range the theoretical interaction curves may be expected to be in reasonable agreement with experimental results because axial tension tends to minimize the effects of initial eccentricities, which are generally considered to be responsible for the large discrepancies between the theoretical and the experimental values of critical compressive stress. Therefore, under combined torsion and moderate tension - that is, the tension range for which computed results are available - a conservative approximation to the buckling stress which may be used for the design of cylinders of moderate or large curvature is a straight line. This straight line has the same slope as the theoretical interaction curve in the tension range and passes through the point corresponding to buckling of a cylinder in torsion alone as obtained from the empirical curve of figure 3.

#### INTERACTION FORMULAS

On the basis of the preceding discussion of the interaction curves, the critical combinations of torsion and direct axial stress for thin-walled cylinders of moderate or large curvature may be expressed approximately in stress-ratio form by the following simple formulas.

Theoretical interaction formulas.- Theoretical interaction formulas for  $30 < Z < 7.7 \frac{r^2}{t^2}$  can be expressed by the following

equations: for shear and compression  $(0 < (R_x)_{th} < 1)$ ,

$$(R_s)_{th} + (R_x)_{th} = 1 \quad (1)$$

and for shear and moderate tension  $(-1 \lesssim (R_x)_{th} < 0)$ ,

$$(R_s)_{th} + 0.8(R_x)_{th} = 1 \quad (2)$$



The theoretical critical stresses of cylinders in torsion alone and cylinders in axial compression alone can be obtained by the use of figures 3 and 4, respectively. Figure 2 shows that equations (1) and (2) are fairly good approximations to the theoretical results.

Empirical interaction formulas.— Empirical interaction formulas can be expressed by the following equations: for shear and compression  $(0 < (R_x)_{\text{exp}} < 1)$ ,

$$(R_s)_{\text{exp}}^2 + (R_x)_{\text{exp}} = 1 \quad (3)$$

and for shear and moderate tension  $(-1 \lesssim (R_x)_{\text{th}} < 0)$ ,

$$(R_s)_{\text{th}} + 0.8(R_x)_{\text{th}} = 0.9 \quad (4)$$

Equation (3) is valid when  $1 < Z < 7.7 \frac{r^2}{t^2}$  for cylinders with simply supported edges and when  $5 < Z < 7.7 \frac{r^2}{t^2}$  for cylinders with clamped edges; equation (4) is valid when  $30 < Z < 7.7 \frac{r^2}{t^2}$  for cylinders with both simply supported and clamped edges.

The empirical critical stresses of cylinders in torsion alone and cylinders in axial compression alone can be obtained by the use of figures 3 and 4, respectively. At values of  $Z < 30$  the theoretical solution may be used for design purposes in the tension range.

#### COMPARISON OF EMPIRICAL INTERACTION RESULTS WITH TEST

##### DATA FROM OTHER INVESTIGATIONS

The accuracy of the empirical results is checked by a comparison with test data in figures 5 and 6. In figure 5 test data obtained from reference 3 for celluloid cylinders are given for several

selected values of  $Z$ . Each cylinder was buckled several times under different combinations of torsion and axial stress and the results are presented directly in stress-ratio form. These stress ratios are based upon the observed critical stresses of the cylinder in torsion alone and in axial compression alone and therefore the results serve as a check only on the shape of the interaction curve and not on the actual stresses. In figure 5 the assumption of a parabolic interaction curve is shown to be slightly conservative. The parabolic interaction curve in figure 5 corresponds to the more conservative of two formulas suggested in reference 3 by Bruhn and is the same as the formula suggested by Ballerstedt and Wagner (reference 5) for the compression range.

Test data for several values of  $Z$  obtained by Bridget in reference 4 for the buckling of brass and steel cylinders under combined torsion and axial stress are plotted in stress-ratio form in figure 6. Because a different cylinder was used for each combination of loads, the data show considerably more scatter than those of reference 3. The reduction of the data from stresses to stress ratios by the use of the empirical curves of figures 3 and 4, however, provides a check on the accuracy of the points corresponding to shear alone and compression alone which is not provided by the test data of reference 3. The empirical interaction curve, also shown in figure 6, lies near the center of the rather wide scatter band.

Ballerstedt and Wagner (reference 5) tested a number of very thin brass cylinders under combined torsion and tension and concluded that for the design of cylinders under such loading conditions the following equation may be used:

$$\left(R_s\right)_{\text{exp}} + 0.5\left(R_x\right)_{\text{exp}} = 1 \quad (5)$$

Results obtained by use of equation (5) appear to be in very satisfactory agreement with experimental results when the equation is used in conjunction with the formulas given in reference 5 for buckling in pure compression and pure tension; when equation (5) is used in conjunction with the more accurate values given in figures 3 and 4, however, the equation is very

unconservative. The test data of reference 5 compare favorably with the present recommended design curves when the stress ratios are recomputed by use of the empirical critical stresses given in figures 3 and 4.

Langley Memorial Aeronautical Laboratory  
National Advisory Committee for Aeronautics  
Langley Field, Va., March 20, 1947

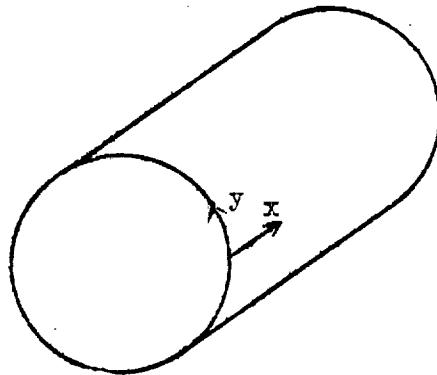
## APPENDIX A

## THEORETICAL SOLUTION

Equation of equilibrium.- The combinations of shear and axial stress which will cause a cylinder to buckle may be obtained by solving the following equation of equilibrium (see reference 7):

$$D\nabla^4 w + \frac{Et}{r^2} \nabla^{-4} \frac{\partial^4 w}{\partial x^4} + 2\tau t \frac{\partial^2 w}{\partial x \partial y} + \sigma_x t \frac{\partial^2 w}{\partial x^2} = 0 \quad (A1)$$

where  $x$  and  $y$  are the coordinates indicated in the following figure:



Division of equation (A1) by  $D$  gives the equation

$$\nabla^4 w + \frac{12Z^2}{L^4} \nabla^{-4} \frac{\partial^4 w}{\partial x^4} + 2k_s \frac{\pi^2}{L^2} \frac{\partial^2 w}{\partial x \partial y} + k_x \frac{\pi^2}{L^2} \frac{\partial^2 w}{\partial x^2} = 0 \quad (A2)$$

where the dimensionless parameters  $Z$ ,  $k_s$ , and  $k_x$  are defined by

$$Z = \frac{L^2}{rt} \sqrt{1 - \mu^2}$$

$$k_s = \frac{rtL^2}{D\pi^2}$$

$$k_x = \frac{\sigma_x t L^2}{D\pi^2}$$

Equation (A2) can be represented by

$$Qw = 0 \tag{A3}$$

where  $Q$  is defined by

$$Q = \nabla^4 + \frac{12Z^2}{L^4} \nabla^{-4} \frac{\partial^4}{\partial x^4} + 2k_s \frac{\pi^2}{L^2} \frac{\partial^2}{\partial x \partial y} + k_x \frac{\pi^2}{L^2} \frac{\partial^2}{\partial x^2}$$

Method of solution.- Equation (A3) may be solved by using the Galerkin method as given in reference 8. In the application of this method, equation (A3) is solved by the use of a suitable series expansion for  $w$  as follows:

$$w = \sum_{m=1}^J a_m V_m + \sum_{m=1}^J b_m W_m \tag{A4}$$

In equation (A4) the functions  $V_1, V_2 \dots V_J, W_1, W_2 \dots W_J$  individually satisfy the boundary conditions on  $w$  but need not satisfy the equation of equilibrium.

The coefficients  $a_m$  and  $b_m$  are then determined by the equations

$$\left. \begin{aligned} \int_0^{2\lambda} \int_0^b V_n Q w \, dx \, dy &= 0 \\ \int_0^{2\lambda} \int_0^b W_n Q w \, dx \, dy &= 0 \end{aligned} \right\} \quad (A5)$$

where  $n = 1, 2, 3, \dots$

The boundary conditions considered in the present paper are as follows: For simply supported edges,

$$w = \frac{\partial^2 w}{\partial x^2} = v = 0, \text{ and } u \text{ is unrestrained;}$$

and for clamped edges,

$$w = \frac{\partial w}{\partial x} = u = 0, \text{ and } v \text{ is unrestrained.}$$

Solution for cylinders with simply supported edges.- The following infinite series expansion can be used to represent exactly the displacement  $w$  in the case of cylinders with simply supported edges:

$$w = \sin \frac{\pi Y}{\lambda} \sum_{m=1}^{\infty} a_m \sin \frac{m\pi X}{L} + \cos \frac{\pi Y}{\lambda} \sum_{m=1}^{\infty} b_m \sin \frac{m\pi X}{L} \quad (A6)$$

where  $\lambda$  is the half wave length of the buckles in the circumferential direction. Expression (A6) is equivalent to equation (A4) if

$$\left. \begin{aligned} V_n &= \sin \frac{\pi Y}{\lambda} \sin \frac{n\pi X}{L} \\ W_n &= \cos \frac{\pi Y}{\lambda} \sin \frac{n\pi X}{L} \end{aligned} \right\} \quad (A7)$$

Substitution of expressions (A6) and (A7) into equations (A5) and integration over the limits indicated give

$$\left. \begin{aligned} a_n \left[ (n^2 + \beta^2)^2 + \frac{12Z^2 n^4}{\pi^4 (n^2 + \beta^2)^2} - n^2 k_x \right] - \frac{8\beta k_s}{\pi} \sum_{m=1}^{\infty} b_m \frac{mn}{n^2 - m^2} = 0 \\ b_n \left[ (n^2 + \beta^2)^2 + \frac{12Z^2 n^4}{\pi^4 (n^2 + \beta^2)^2} - n^2 k_x \right] + \frac{8\beta k_s}{\pi} \sum_{m=1}^{\infty} a_m \frac{mn}{n^2 - m^2} = 0 \end{aligned} \right\} \quad (A8)$$

where

$$\beta = \frac{L}{\lambda}$$

$$n = 1, 2, 3, \dots$$

Equations (A8) have a solution in which the coefficients  $a_n$  and the coefficients  $b_n$  are not all zero only if the following determinant vanishes:

	a <sub>1</sub>	a <sub>2</sub>	a <sub>3</sub>	a <sub>4</sub>	a <sub>5</sub>	a <sub>6</sub>	...	b <sub>1</sub>	b <sub>2</sub>	b <sub>3</sub>	b <sub>4</sub>	b <sub>5</sub>	b <sub>6</sub>	...
n=1	$\frac{1}{k_B} M_1$	0	0	0	0	0	...	0	$\frac{2}{3}$	0	$\frac{4}{15}$	0	$\frac{6}{35}$	...
n=2	0	$\frac{1}{k_B} M_2$	0	0	0	0	...	$-\frac{2}{3}$	0	$\frac{6}{5}$	0	$\frac{10}{21}$	0	...
n=3	0	0	$\frac{1}{k_B} M_3$	0	0	0	...	0	$-\frac{6}{5}$	0	$\frac{12}{7}$	0	$\frac{2}{3}$	...
n=4	0	0	0	$\frac{1}{k_B} M_4$	0	0	...	$-\frac{4}{15}$	0	$-\frac{12}{7}$	0	$\frac{20}{9}$	0	...
n=5	0	0	0	0	$\frac{1}{k_B} M_5$	0	...	0	$-\frac{10}{21}$	0	$-\frac{20}{9}$	0	$\frac{30}{11}$	...
n=6	0	0	0	0	0	$\frac{1}{k_B} M_6$	...	$-\frac{6}{35}$	0	$-\frac{2}{3}$	0	$-\frac{30}{11}$	0	...
	⋮	⋮	⋮	⋮	⋮	⋮		⋮	⋮	⋮	⋮	⋮	⋮	
n=1	0	$-\frac{2}{3}$	0	$-\frac{4}{15}$	0	$-\frac{6}{35}$	...	$\frac{1}{k_B} M_1$	0	0	0	0	0	...
n=2	$\frac{2}{3}$	0	$-\frac{6}{5}$	0	$-\frac{10}{21}$	0	...	0	$\frac{1}{k_B} M_2$	0	0	0	0	...
n=3	0	$\frac{6}{5}$	0	$-\frac{12}{7}$	0	$-\frac{2}{3}$	...	0	0	$\frac{1}{k_B} M_3$	0	0	0	...
n=4	$\frac{4}{15}$	0	$\frac{12}{7}$	0	$-\frac{20}{9}$	0	...	0	0	0	$\frac{1}{k_B} M_4$	0	0	...
n=5	0	$\frac{10}{21}$	0	$\frac{20}{9}$	0	$-\frac{30}{11}$	...	0	0	0	0	$\frac{1}{k_B} M_5$	0	...
n=6	$\frac{6}{35}$	0	$\frac{2}{3}$	0	$\frac{30}{11}$	0	...	0	0	0	0	0	$\frac{1}{k_B} M_6$	...
	⋮	⋮	⋮	⋮	⋮	⋮		⋮	⋮	⋮	⋮	⋮	⋮	

(A9)





The first approximation, obtained from the second-order determinant, is given by

$$k_s^2 = \left(\frac{3}{2}\right)^2 M_1 M_2 \quad (A11)$$

The second approximation, obtained from the third-order determinant, is given by

$$k_s^2 = \frac{M_1 M_2 M_3}{\left(\frac{6}{5}\right)^2 M_1 + \left(\frac{2}{3}\right)^2 M_3} \quad (A12)$$

The third approximation, obtained from the fourth-order determinant, is given by

$$k_s^4 \left(\frac{8}{7} + \frac{8}{25}\right)^2 - k_s^2 \left[ \left(\frac{12}{7}\right)^2 M_1 M_2 + \left(\frac{6}{5}\right)^2 M_1 M_4 + \left(\frac{4}{15}\right)^2 M_2 M_3 + \left(\frac{2}{3}\right)^2 M_3 M_4 \right] + M_1 M_2 M_3 M_4 = 0 \quad (A13)$$

The shear-stress coefficient  $k_s$  may be found in the various approximations directly from equations (A11), (A12), and (A13) for any given values of  $Z$ ,  $k_x$ , and  $\beta$ . Because a structure buckles at the lowest stress at which instability occurs, the value of  $k_s$  is found for a series of values of  $\beta$ . The minimum value of  $k_s$  for the given values of  $Z$  and  $k_x$  is then determined from a plot of  $k_s$  against  $\beta$ . Table 1 shows the convergence of the various approximations for  $k_s$ .

Solution for cylinders with clamped edges.- A procedure similar to that used for cylinders with simply supported edges may be followed for cylinders with clamped edges. The deflection function used is the following series:

$$\begin{aligned}
 w = & \sin \frac{\pi y}{\tau} \sum_{m=1}^{\infty} a_m \left[ \cos \frac{(m-1)\pi x}{L} - \cos \frac{(m+1)\pi x}{L} \right] \\
 & + \cos \frac{\pi y}{\tau} \sum_{m=1}^{\infty} b_m \left[ \cos \frac{(m-1)\pi x}{L} - \cos \frac{(m+1)\pi x}{L} \right]
 \end{aligned} \tag{A14}$$

Comparison of equation (A14) with equation (A4) shows that

$$\left. \begin{aligned}
 V_n &= \sin \frac{\pi y}{\tau} \left[ \cos \frac{(n-1)\pi x}{L} - \cos \frac{(n+1)\pi x}{L} \right] \\
 W_n &= \cos \frac{\pi y}{\tau} \left[ \cos \frac{(n-1)\pi x}{L} - \cos \frac{(n+1)\pi x}{L} \right]
 \end{aligned} \right\} \tag{A15}$$

where  $n = 1, 2, 3, \dots$

When operations equivalent to those carried out for the case of simply supported edges are performed, the following simultaneous equations result:

(A16)

For  $n = 1$

$$a_1(2M_0 + M_2) - a_3M_2 + k_8 \sum_{m=2,4,6}^{\infty} b_m \left[ -\frac{(m-1)^2}{(m-1)^2 - 4} + \frac{(m+1)^2}{(m+1)^2 - 4} \right] = 0$$

For  $n = 2$

$$a_2(M_1 + M_3) - a_4M_3 + k_9 \sum_{m=1,3,5}^{\infty} b_m \left[ \frac{(m-1)^2}{(m-1)^2 - 1} - \frac{(m-1)^2}{(m-1)^2 - 9} + \frac{(m+1)^2}{(m+1)^2 - 1} + \frac{(m+1)^2}{(m+1)^2 - 9} \right] = 0$$

For  $n = 3, 4, 5, \dots$

$$a_n(M_{n-1} + M_{n+1}) - a_{n-2}M_{n-1} - a_{n+2}M_{n+1} + k_8 \sum_{m=1}^{\infty} b_m \left[ \frac{(m-1)^2}{(m-1)^2 - (n-1)^2} - \frac{(m-1)^2}{(m+1)^2 - (n-1)^2} + \frac{(m+1)^2}{(m+1)^2 - (n-1)^2} + \frac{(m+1)^2}{(m+1)^2 - (n+1)^2} \right] = 0$$

where  $m \pm n$  is odd.

For  $n = 1$

$$b_1(2M_0 + M_2) - b_3M_2 - k_8 \sum_{m=2,4,6}^{\infty} a_m \left[ -\frac{(m-1)^2}{(m-1)^2 - 4} + \frac{(m+1)^2}{(m+1)^2 - 4} \right] = 0$$

For  $n = 2$

$$b_2(M_1 + M_3) - b_4M_3 - k_9 \sum_{m=1,3,5}^{\infty} a_m \left[ \frac{(m-1)^2}{(m-1)^2 - 1} - \frac{(m-1)^2}{(m-1)^2 - 9} + \frac{(m+1)^2}{(m+1)^2 - 1} + \frac{(m+1)^2}{(m+1)^2 - 9} \right] = 0$$

For  $n = 3, 4, 5, \dots$

$$b_n(M_{n-1} + M_{n+1}) - b_{n-2}M_{n-1} - b_{n+2}M_{n+1} - k_8 \sum_{m=1}^{\infty} a_m \left[ \frac{(m-1)^2}{(m-1)^2 - (n-1)^2} - \frac{(m-1)^2}{(m+1)^2 - (n-1)^2} + \frac{(m+1)^2}{(m+1)^2 - (n-1)^2} + \frac{(m+1)^2}{(m+1)^2 - (n+1)^2} \right] = 0$$

where  $m \pm n$  is odd.

and

$$M_n = \frac{\pi}{8\beta} \left[ (n^2 + \beta^2)^2 + \frac{12Z^2 n^4}{\pi^4 (n^2 + \beta^2)^2} - n^2 k_x \right]$$

The infinite determinant formed by these equations can again be rearranged so as to factor into the product of two mutually equivalent infinite subdeterminants. The vanishing of one of these determinants leads to the following equation:

	$a_1$	$b_2$	$a_3$	$b_4$	$a_5$	$b_6$	...
$n=1$	$\frac{1}{k_s}(2M_0+M_2)$	$\frac{32}{15}$	$-\frac{1}{k_s}M_2$	$-\frac{64}{105}$	$0$	$-\frac{32}{315}$	...
$n=2$	$\frac{32}{15}$	$\frac{1}{k_s}(M_1+M_3)$	$-\frac{352}{105}$	$-\frac{1}{k_s}M_3$	$\frac{32}{35}$	$0$	...
$n=3$	$-\frac{1}{k_s}M_2$	$-\frac{352}{105}$	$\frac{1}{k_s}(M_2+M_4)$	$\frac{1472}{315}$	$-\frac{1}{k_s}M_4$	$-\frac{1376}{1155}$	...
$n=4$	$-\frac{64}{105}$	$-\frac{1}{k_s}M_3$	$\frac{1472}{315}$	$\frac{1}{k_s}(M_3+M_5)$	$-\frac{4160}{693}$	$-\frac{1}{k_s}M_5$	...
$n=5$	$0$	$\frac{32}{35}$	$-\frac{1}{k_s}M_4$	$-\frac{4160}{693}$	$\frac{1}{k_s}(M_4+M_6)$	$\frac{9440}{1287}$	...
$n=6$	$-\frac{32}{315}$	$0$	$-\frac{1376}{1155}$	$-\frac{1}{k_s}M_5$	$\frac{9440}{1287}$	$\frac{1}{k_s}(M_5+M_7)$	...
	$\vdots$	$\vdots$	$\vdots$	$\vdots$	$\vdots$	$\vdots$	$\vdots$
	$\vdots$	$\vdots$	$\vdots$	$\vdots$	$\vdots$	$\vdots$	$\vdots$

= 0

(A17)

The first approximation, obtained from the second-order determinant, is given by

$$k_s^2 = \left(\frac{15}{32}\right)^2 (2M_0 + M_2)(M_1 + M_3) \tag{A18}$$

The second approximation, obtained from the third-order determinant, is given by

$$k_s^2 = \frac{(M_1 + M_3) [(2M_0 + M_2)(M_2 + M_4) - M_2^2]}{\left(\frac{32}{15}\right)^2 (M_2 + M_4) - 2\left(\frac{32}{15}\right)\left(\frac{352}{105}\right)M_2 + \left(\frac{352}{105}\right)^2 (2M_0 + M_2)} \quad (A19)$$

The third approximation, obtained from the fourth-order determinant, is given by

$$\begin{aligned} k_s^4 & \left[ \left(\frac{32}{15}\right)\left(\frac{1472}{315}\right) - \left(\frac{352}{105}\right)\left(\frac{64}{105}\right) \right]^2 - k_s^2 \left\{ \left(\frac{1472}{315}\right)^2 (2M_0 + M_2)(M_1 + M_3) \right. \\ & + \left(\frac{352}{105}\right)^2 (2M_0 + M_2)(M_3 + M_5) + \left(\frac{64}{105}\right)^2 (M_1 + M_3)(M_2 + M_4) \\ & + \left(\frac{32}{15}\right)^2 (M_2 + M_4)(M_3 + M_5) - 2\left(\frac{64}{105}\right)\left(\frac{1472}{315}\right)M_2(M_1 + M_3) \\ & - 2\left(\frac{32}{15}\right)\left(\frac{352}{105}\right)M_2(M_3 + M_5) - 2\left(\frac{352}{105}\right)\left(\frac{1472}{315}\right)M_3(2M_0 + M_2) \\ & \left. - 2\left(\frac{32}{15}\right)\left(\frac{64}{105}\right)M_3(M_2 + M_4) + 2\left[\left(\frac{64}{105}\right)\left(\frac{352}{105}\right) + \left(\frac{32}{15}\right)\left(\frac{1472}{315}\right)\right]M_2M_3 \right\} \\ & + \left[ 2M_0(M_2 + M_4) + M_2M_4 \right] \left[ M_1(M_3 + M_5) + M_3M_5 \right] = 0 \quad (A20) \end{aligned}$$

As in the solution for cylinders with simply supported edges, the value of  $k_s$  has to be minimized with respect to  $\beta$  for given values of  $Z$  and  $k_x$ . Table 1 shows the results of the various approximations for  $k_s$ .

Comparison of present solution with previous theoretical solutions. - In figure 7 the solution given by Kromm (reference 9) is compared with the present theoretical solution for cylinders with simply supported edges. Although the values shown for Kromm's solution are obtained from small-scale curves and are therefore approximate, good agreement is indicated between the results of reference 9 and the present solution.

In figures 8(a) and 8(b) the results of the present paper are compared with those of Leggett (reference 10). The large discrepancies seen in figures 8(a) and 8(b) are believed mainly due to the erroneous assumption in reference 10 that the theoretical interaction curves are parabolic and - in the case of figure 8(b) - to the further erroneous assumption in reference 10 that the cross sections of cylinders with clamped edges in axial compression remain circular.

## APPENDIX B

## VERTICAL PARTS OF THEORETICAL INTERACTION CURVES

At low values of the curvature parameter  $Z$  the theoretical interaction curves have vertical parts at a value of  $k_x$  corresponding to buckling in axial compression alone. (See figs. 1(a) and 1(b).) These vertical parts indicate that some shear stress may be applied to cylinders at low values of  $Z$  without any reduction of the compressive stress necessary to cause buckling. The value of  $Z$  at which the vertical parts of the interaction curves disappear is the upper limit of the range of  $Z$  for which substitution of the value of  $k_x$  for pure compression into the expression for  $k_s$  leads to real values other than zero for  $k_s$ .

Cylinders with simply supported edges.- Equation (A1) represents the first approximation of the critical combinations of shear-stress and axial-stress coefficients for cylinders with simply supported edges. When  $k_s$  is equal to zero, the minimum value of  $k_x$  which satisfies the resulting equation is found by setting  $M_1$  equal to zero and is given by

$$k_x = (1 + \beta^2)^2 + \frac{12Z^2}{\pi^4(1 + \beta^2)^2} \quad (B1)$$

This equation is also obtained as the exact solution for a simply supported cylinder buckling in pure axial compression (reference 2). The buckle pattern corresponding to the lowest buckling load at low values of  $Z$  is that for which  $\beta = 0$ . The substitution of  $\beta = 0$  into equation (B1) results in

$$k_x = 1 + \frac{12Z^2}{\pi^4} \quad (B2)$$

One critical combination of stress coefficients at low values of  $Z$  is therefore



$$\left. \begin{aligned} k_x &= 1 + \frac{12Z^2}{\pi^4} \\ k_s &= 0 \end{aligned} \right\} \quad (B3)$$

Another approximate critical value of  $k_s$  can be found for

$$k_x = 1 + \frac{12Z^2}{\pi^4}$$

by substituting this value of  $k_x$  into equation (A11) and by letting  $\beta$  approach 0. The value of  $k_s$  for the foregoing value of  $k_x$  is

$$k_s^2 = 6 \left( \frac{3\pi}{16} \right)^2 \left( 1 - \frac{12Z^2}{\pi^4} \right) \left( 4 - \frac{12Z^2}{\pi^4} \right) \quad (B4)$$

From equation (B4) it appears that, when  $k_x$  has the value indicated in equations (B3),  $k_s$  depends upon  $Z$  in the following manner: for values of  $Z < \frac{\pi^2}{\sqrt{12}}$ ,  $k_s = \pm \text{Constant}$ ; for values of  $Z = \frac{\pi^2}{\sqrt{12}}$ ,  $k_s = 0$ ; and for values of  $Z > \frac{\pi^2}{\sqrt{12}}$ ,  $k_s$  is imaginary.

Comparison of these values with equations (B3) indicates that the interaction curves have vertical parts for values of  $Z$  in the range

$$Z < \frac{\pi^2}{\sqrt{12}} \quad (B5)$$

Similar calculations with higher approximations for  $k_s$  give the same range of  $Z$  for this vertical part so that expression (B5) may be considered exact.

Cylinders with clamped edges.- An analysis for cylinders with clamped edges similar to that used for cylinders with simply supported edges indicates that the first approximation for the interaction curves gives vertical parts for

$$z < \frac{2\pi^2}{\sqrt{3}} \quad (B6)$$

Expression (B6), unlike expression (B5), is not exact. Because the first approximation, however, is very close to the exact solution when a substantial amount of compression and little shear are present, expression (B5) represents a good approximation to the exact result.

## REFERENCES

1. Batdorf, S. B., Stein, Manuel, and Schildcrout, Murry: Critical Stress of Thin-Walled Cylinders in Torsion. NACA TN No. 1344, 1947.
2. Batdorf, S. B., Schildcrout, Murry, and Stein, Manuel: Critical Stress of Thin-Walled Cylinders in Axial Compression. NACA TN No. 1343, 1947.
3. Bruhn, Elmer, F.: Tests on Thin-Walled Celluloid Cylinders to Determine the Interaction Curves under Combined Bending, Torsion, and Compression or Tension Loads. NACA TN No. 951, 1945.
4. Bridget, F. J., Jerome, C. C., and Vosseller, A. B.: Some New Experiments on Buckling of Thin-Wall Construction. Trans. A.S.M.E., APM-56-6, vol. 56, no. 8, Aug. 1934, pp. 569-578.
5. Ballerstedt, W., and Wagner, H.: Versuche über die Festigkeit dünner unversteifter Zylinder unter Schub- und Längskräften. Luftfahrtforschung, Bd. 13, Nr. 9, Sept. 20, 1936, pp. 309-312.
6. Batdorf, S. B., and Houbolt, John C.: Critical Combinations of Shear and Transverse Direct Stress for an Infinitely Long Flat Plate with Edges Elastically Restrained against Rotation. NACA ARR No. L4L14, 1945.
7. Batdorf, S. B.: A Simplified Method of Elastic-Stability Analysis for Thin Cylindrical Shells. II - Modified Equilibrium Equation. NACA TN No. 1342, 1947.
8. Duncan, W. J.: The Principles of the Galerkin Method. R. & M. No. 1848, British A.R.C., 1938.
9. Kromm, A.: Knickfestigkeit gekrümmter Platten unter gleichzeitiger Wirkung von Schub- und Längskräften. Bericht 119 der Lillienthal-Gesellschaft für Luftfahrtforschung, 1939.
10. Leggett, D. M. A.: The Initial Buckling of Slightly Curved Panels under Combined Shear and Compression. R. & M. No. 1972, British A.R.C., 1943.

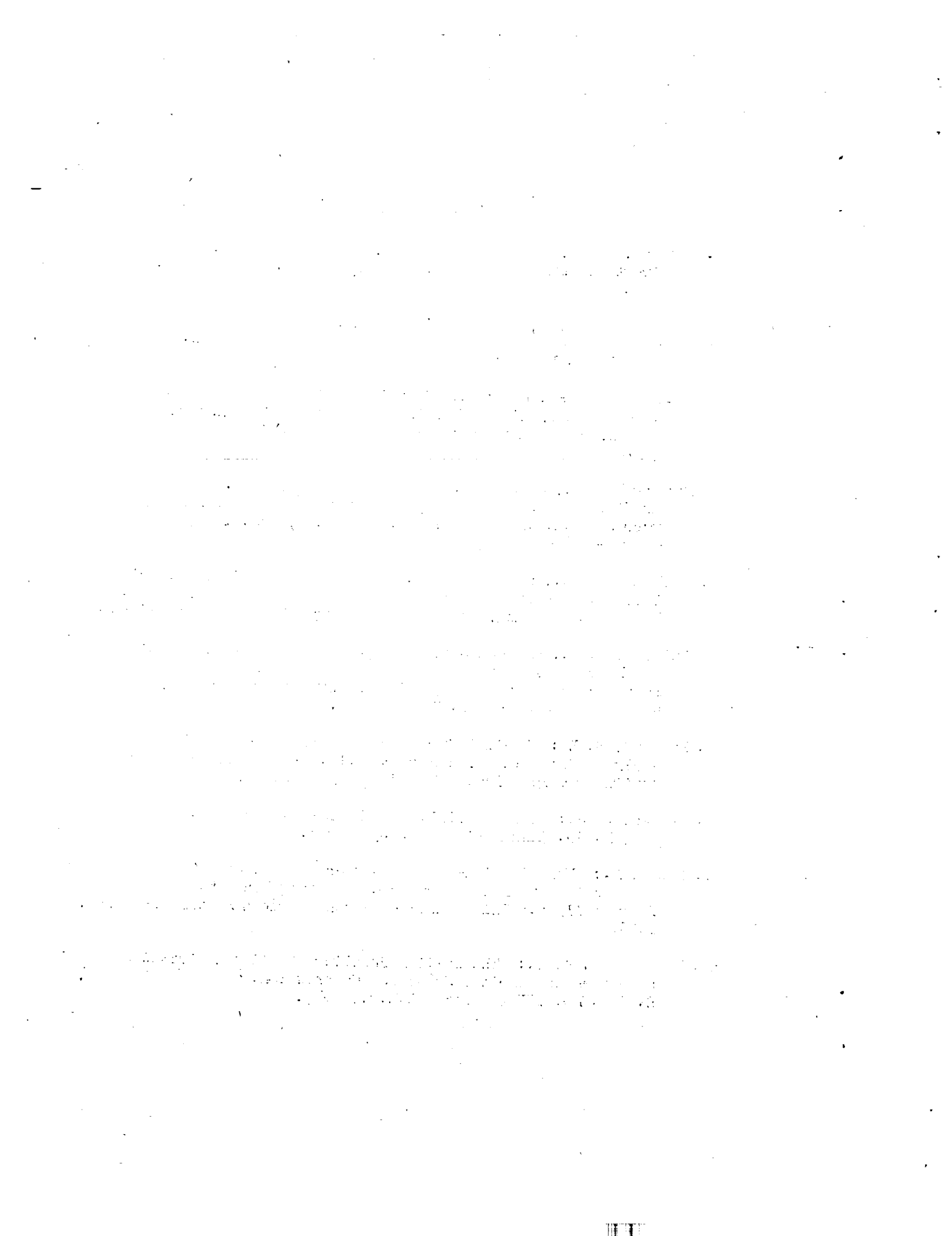


TABLE I

THEORETICAL COMBINATIONS OF SHEAR-STRESS AND AXIAL-STRESS  
COEFFICIENTS AND WAVE LENGTHS OF BUCKLES

Z	$k_x$	First approximation		Second approximation		Third approximation	
		$k_s$	$\beta$	$k_s$	$\beta$	$k_s$	$\beta$
Cylinders with simply supported edges							
1	-1	-----	----	6.64	0.94	-----	-----
	0	-----	----	5.42	.86	5.41	0.365
	.7	-----	----	4.26	.64	-----	-----
	1.12	2.65	0	-----	-----	-----	-----
	1.12	0	0	-----	-----	-----	-----
5	-2	8.9	1.15	8.12	1.16	8.10	1.2
	-1	7.84	1.07	7.21	1.1	-----	-----
	1	5.40	.89	5.11	.92	-----	-----
	2	4.00	.80	3.82	.80	-----	-----
	2.5	3.12	.75	3.04	.75	-----	-----
	3	2.11	.67	2.09	.67	-----	-----
	3.33	1.21	.62	1.20	.62	-----	-----
10	-4	11.95	1.4	10.57	1.42	10.57	1.42
	-2	10.2	1.32	9.1	1.35	-----	-----
	2	6.36	1.15	5.83	1.16	-----	-----
	4	4.21	1.06	3.95	1.06	-----	-----
	5	3.04	1.0	2.90	1.02	-----	-----
	6	1.78	.97	1.75	.96	-----	-----
	6.66	.88	.92	.86	.93	-----	-----



TABLE 1 - Continued

THEORETICAL COMBINATIONS OF SHEAR-STRESS AND AXIAL-STRESS  
 COEFFICIENTS AND WAVE LENGTHS OF BUCKLES - Continued

Z	$k_x$	First approximation		Second approximation		Third approximation	
		$k_s$	$\beta$	$k_s$	$\beta$	$k_s$	$\beta$
Cylinders with simply supported edges							
30	-10	21.20	1.95	17.88	2.02	17.5	2.3
	-5	18.12	1.9	15.33	1.95	15.31	2.0
	5	11.62	1.75	9.93	1.78	-----	-----
	10	8.18	1.68	7.04	1.71	-----	-----
	15	4.59	1.6	4.00	1.6	-----	-----
	18	2.36	1.55	2.09	1.55	-----	-----
	20	.84	1.53	.77	1.53	-----	-----
100	-40	51.0	2.9	41.7	3.1	41.0	3.3
	-20	42.5	2.8	34.9	3.2	34.6	3.1
	20	25.2	2.7	20.8	2.9	-----	-----
	40	16.2	2.6	13.2	2.75	-----	-----
	60	6.8	2.6	5.33	2.7	-----	-----
	65	4.5	2.6	3.0	2.7	-----	-----
	66.6	3.5	2.6	2.2	2.8	-----	-----
1000	-400	277.0	5.55	224.2	6.2	220.66	6.5
	-200	233.5	5.5	189.5	6.1	186.4	6.35
	200	144.8	5.3	117.2	5.95	114.56	6.4
	400	99.0	5.25	78.5	6.00	-----	-----
	500	75.6	5.25	58.2	6.00	-----	-----
	600	51.1	5.45	35.8	6.1	-----	-----
	650	36.2	5.6	23.2	6.1	-----	-----
	666	30.0	5.65	18.65	5.95	15.25	7.0

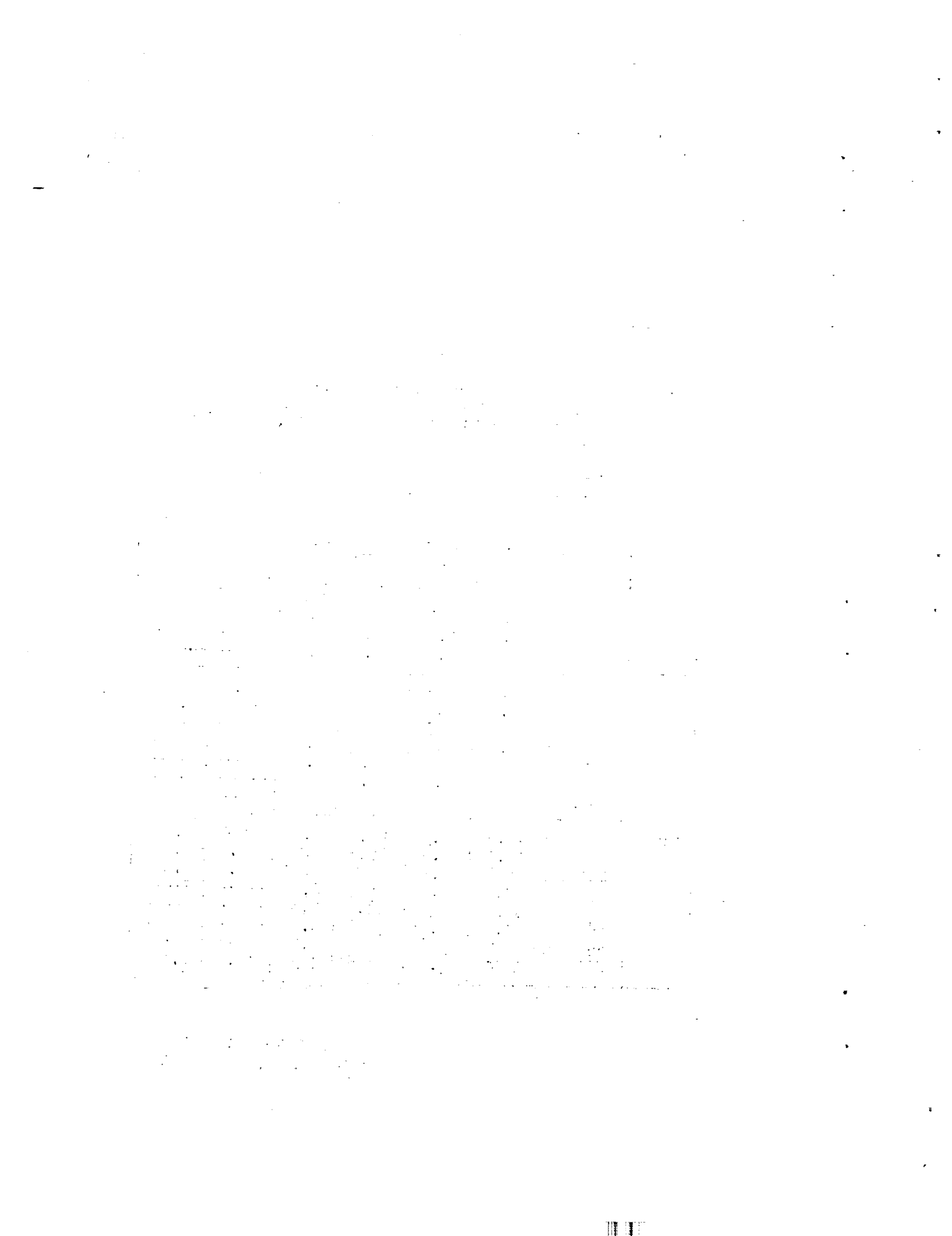
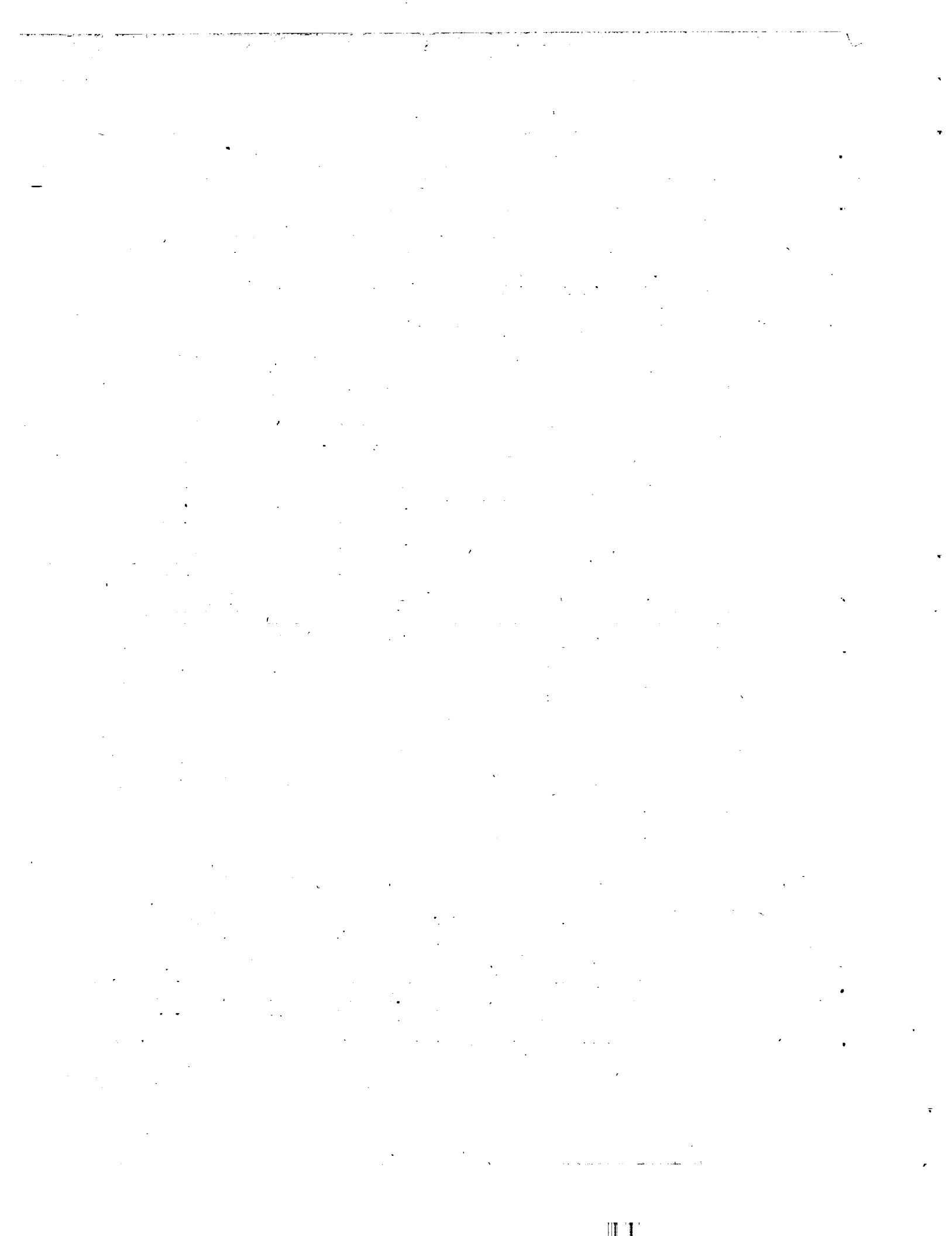


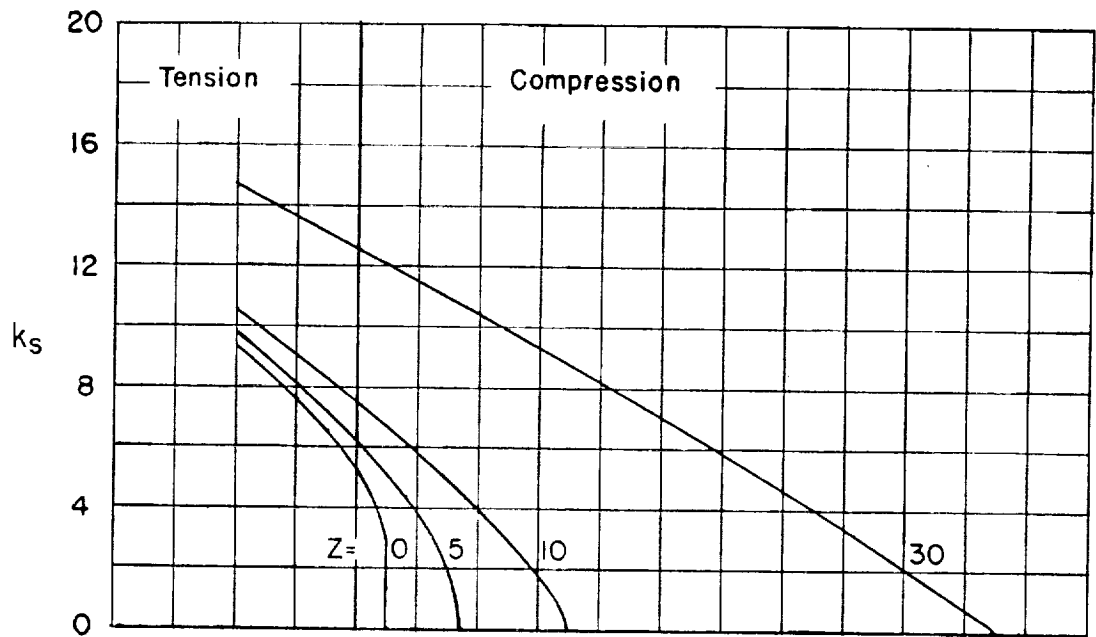


TABLE 1 - Concluded

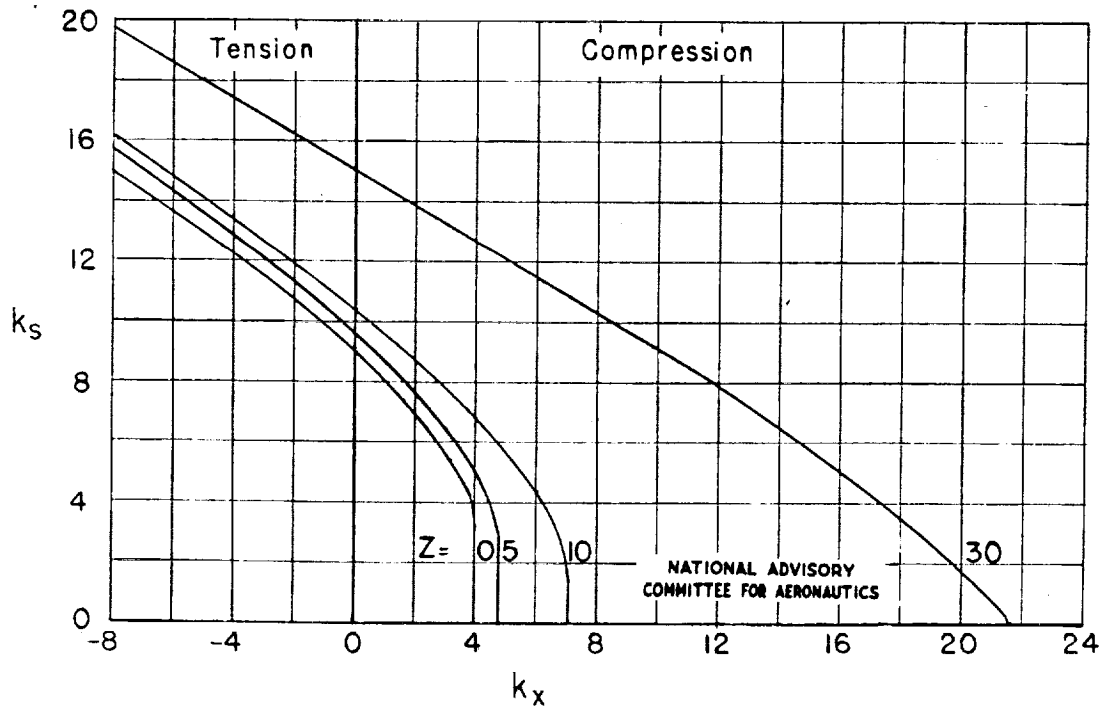
THEORETICAL COMBINATIONS OF SHEAR-STRESS AND AXIAL-STRESS  
 COEFFICIENTS AND WAVE LENGTHS OF BUCKLES - Concluded

z	k <sub>x</sub>	First approximation		Second approximation	
		k <sub>s</sub>	β	k <sub>s</sub>	β
Cylinders with clamped edges					
1	-4.0	13.15	2.0	12.66	2.17
	3.0	6.02	.7	5.96	.715
	3.7	4.75	.41	4.73	.415
	3.9	4.20	.26	4.19	.275
	4.1	3.36	0	-----	-----
	4.1	0	0	-----	-----
2	-4.0	13.18	2.03	12.69	2.19
	3.0	6.11	.72	6.04	.76
	3.7	4.91	.45	4.88	.47
	4.0	4.13	.255	4.12	.26
	4.2	3.32	0	-----	-----
	4.2	0	0	-----	-----
5	-5	14.17	2.24	13.59	2.4
	3	6.66	.95	6.56	.97
	4.2	4.86	.55	4.82	.55
	4.8	3.01	0	-----	-----
	4.8	0	0	-----	-----
	10	-6	15.52	2.6	14.79
4		6.96	1.2	6.82	1.25
6		4.47	.75	4.43	.76
7.2		1.50	0	-----	-----
7.2		0	0	-----	-----
30		-20	27.54	4.90	25.44
	14	6.70	2.46	6.25	2.60
	18	3.60	2.15	3.34	2.25
	21.5	0	1.28	-----	-----





(a) Simply supported edges.



(b) Clamped edges.

Figure 1.- Theoretical combinations of shear-stress and axial-stress coefficients for buckling of cylinders.

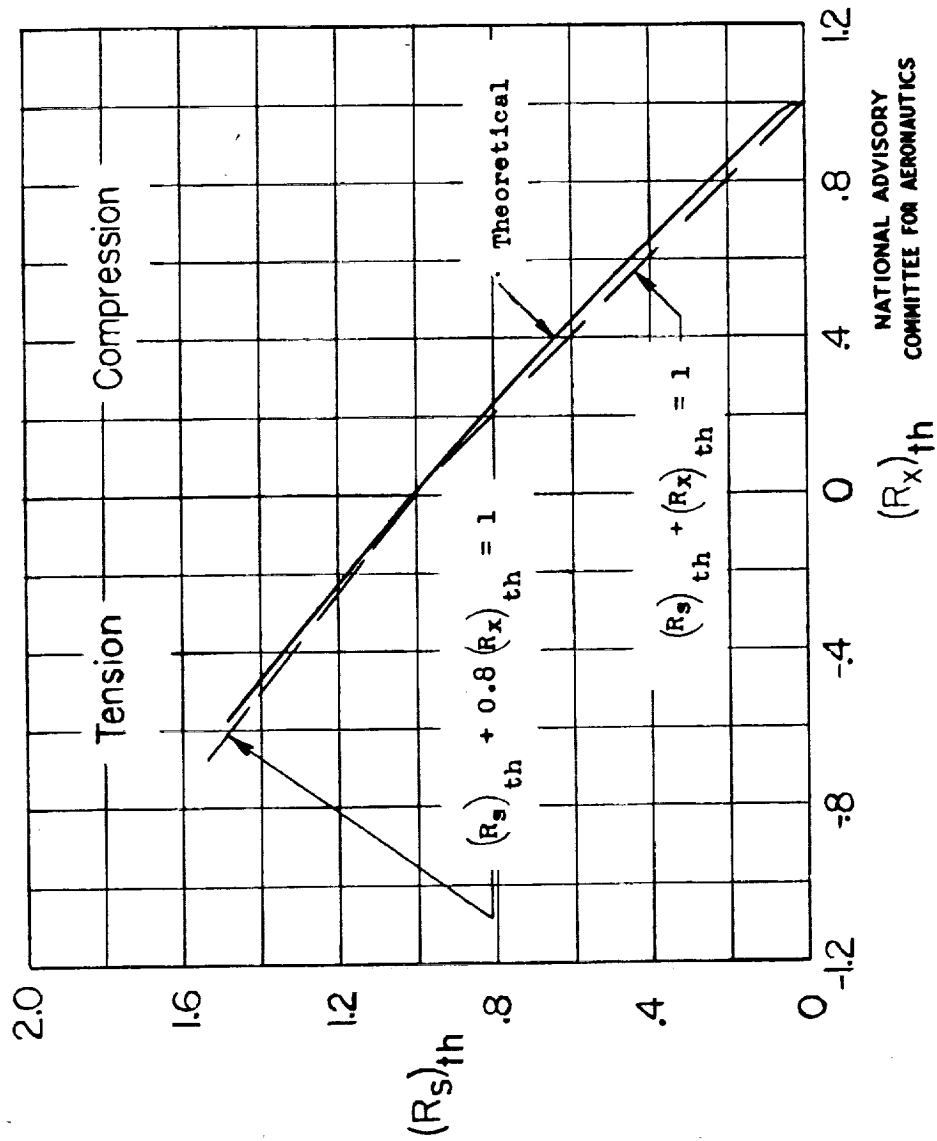


Figure 2.- Comparison of approximate theoretical interaction equation and present solution for  $Z > 30$ .

30

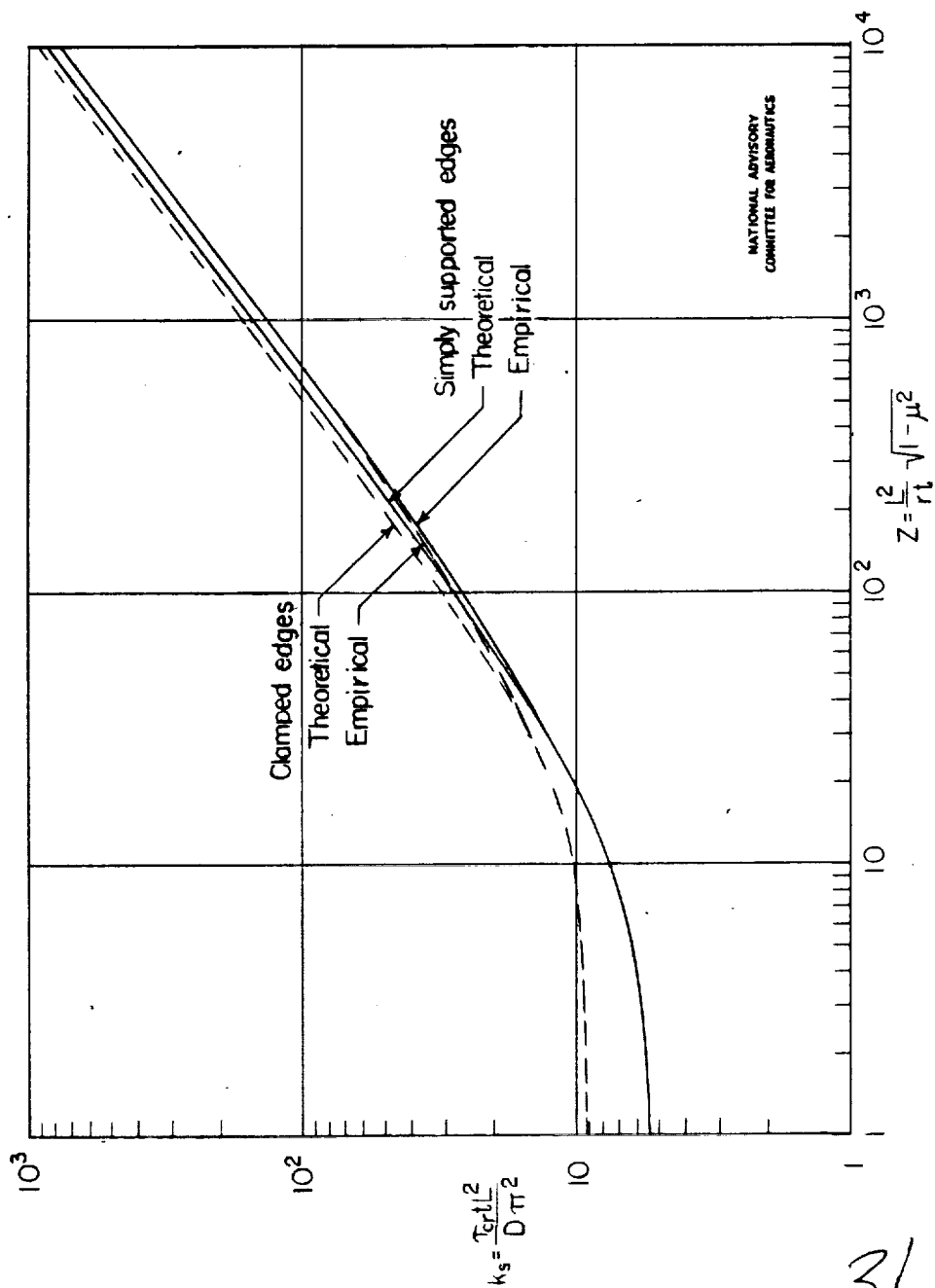


Figure 3.- Critical stress coefficients for buckling of cylinders in torsion.

31

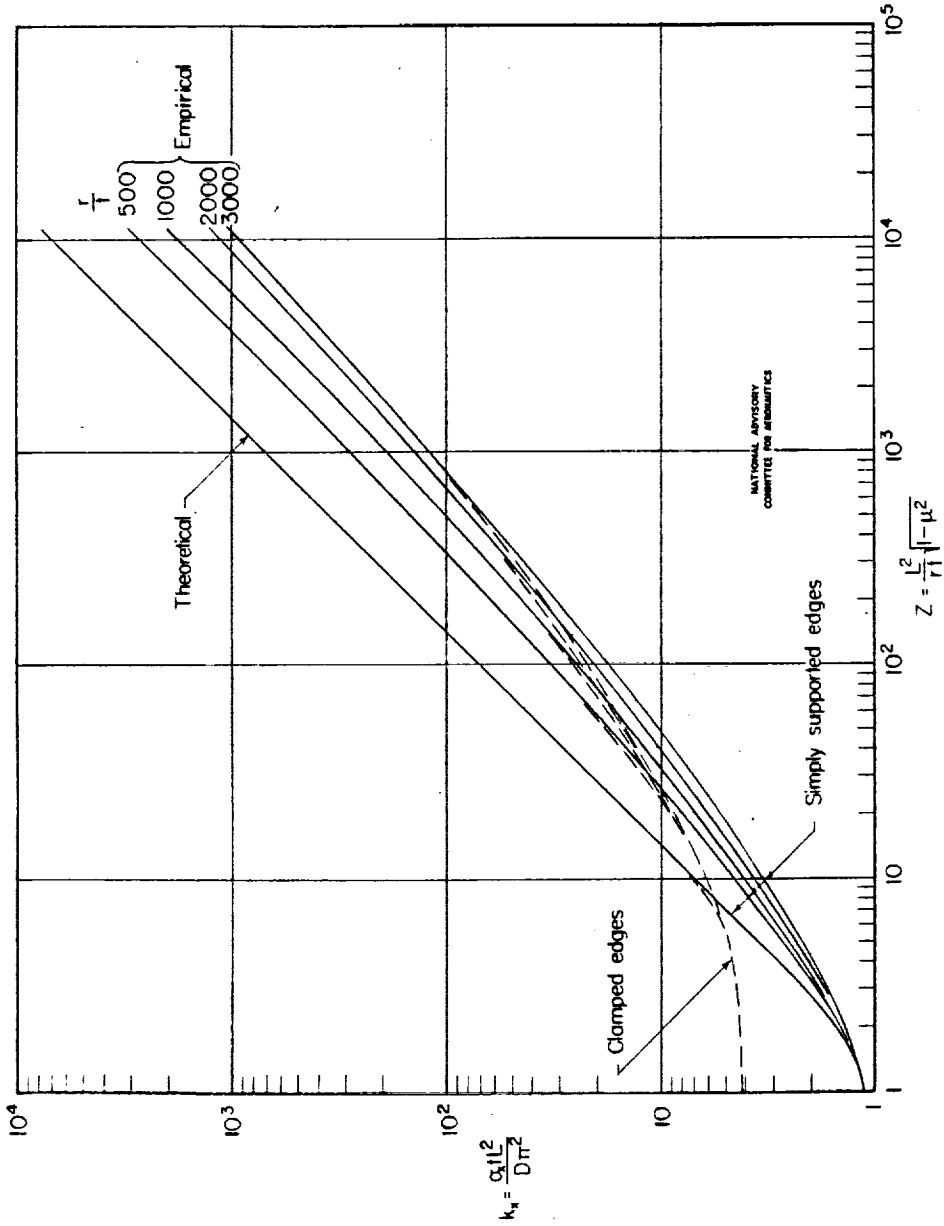


Figure 4.- Critical stress coefficients for buckling of cylinders in axial compression.

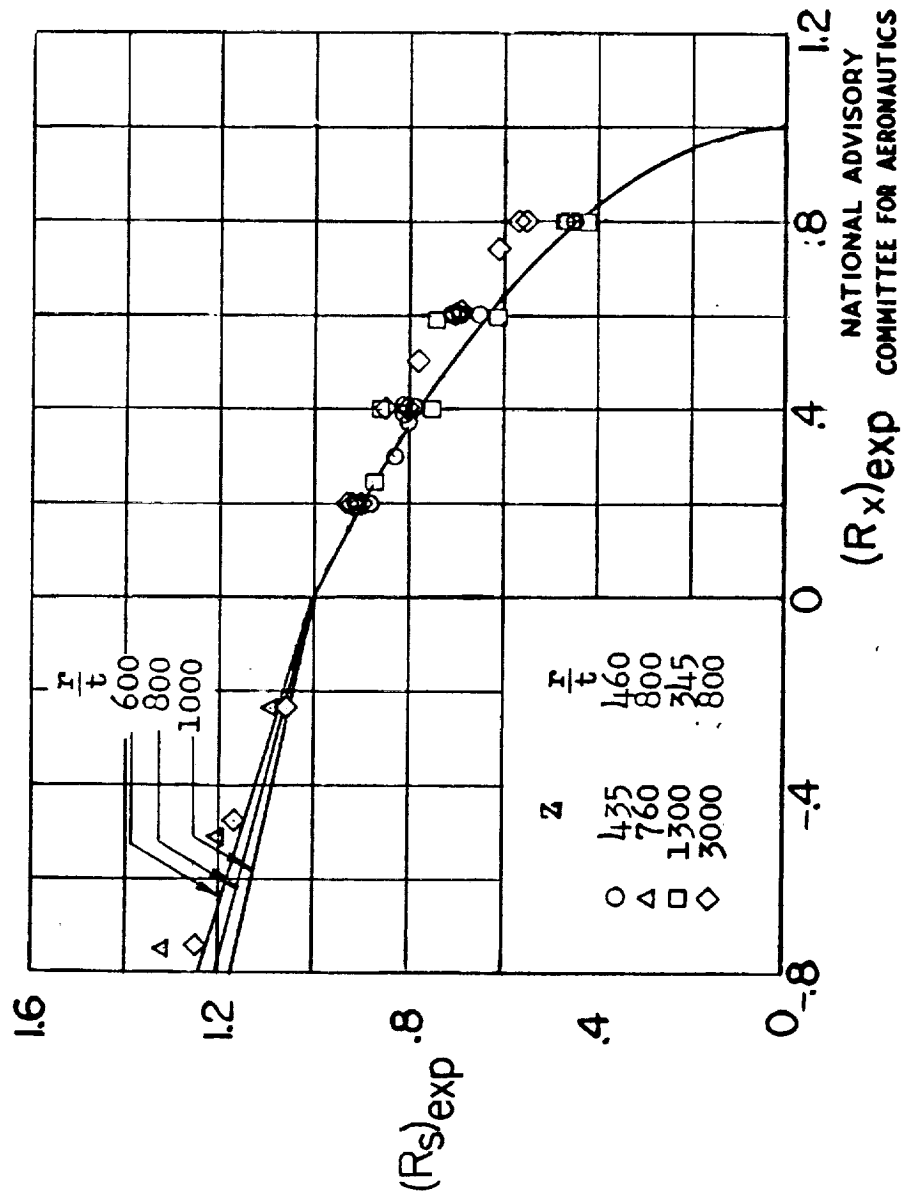


Figure 5.- Comparison of empirical interaction curve with test data presented by Bruhn.

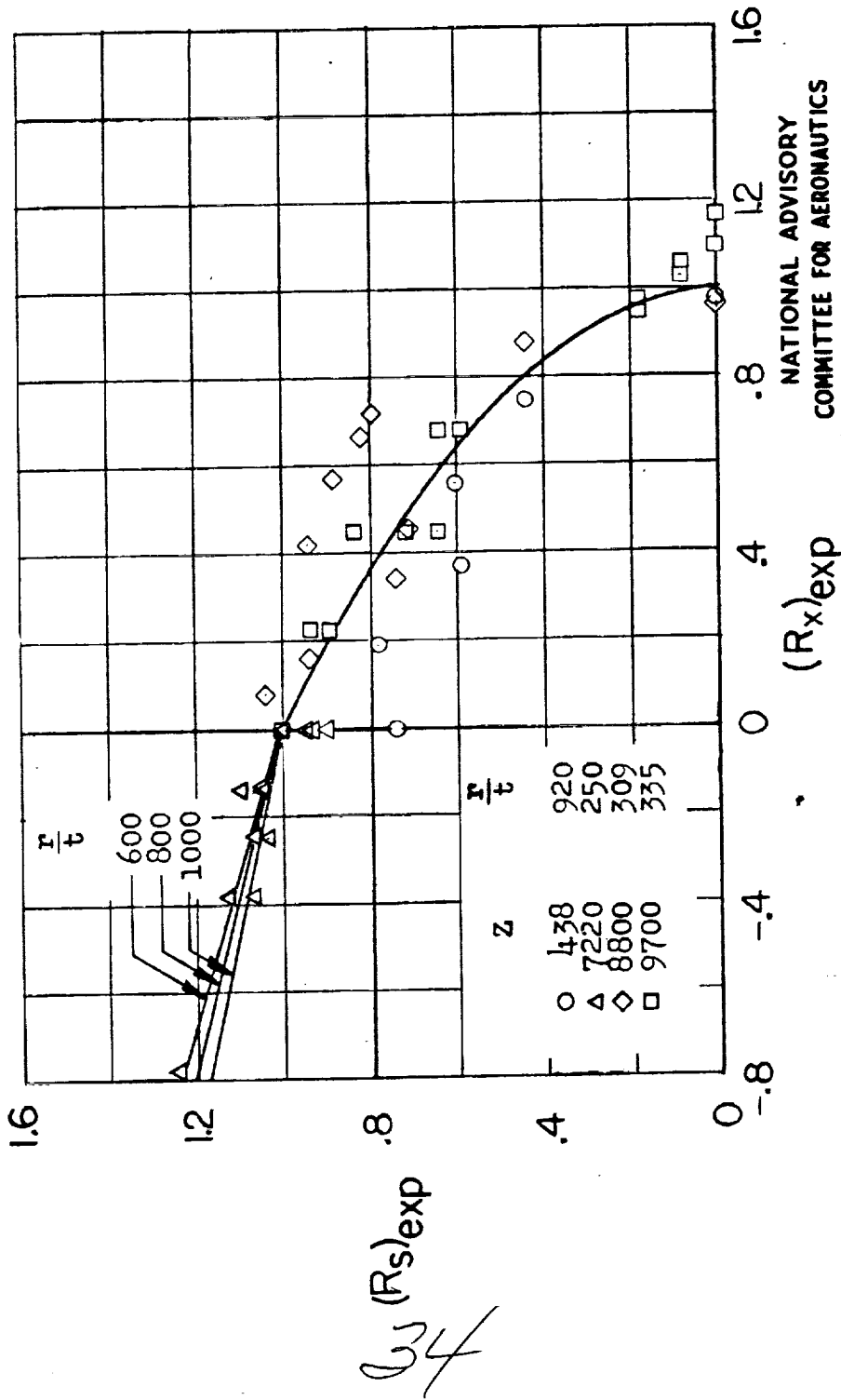


Figure 6.- Comparison of empirical interaction curve with test data presented by Bridget.



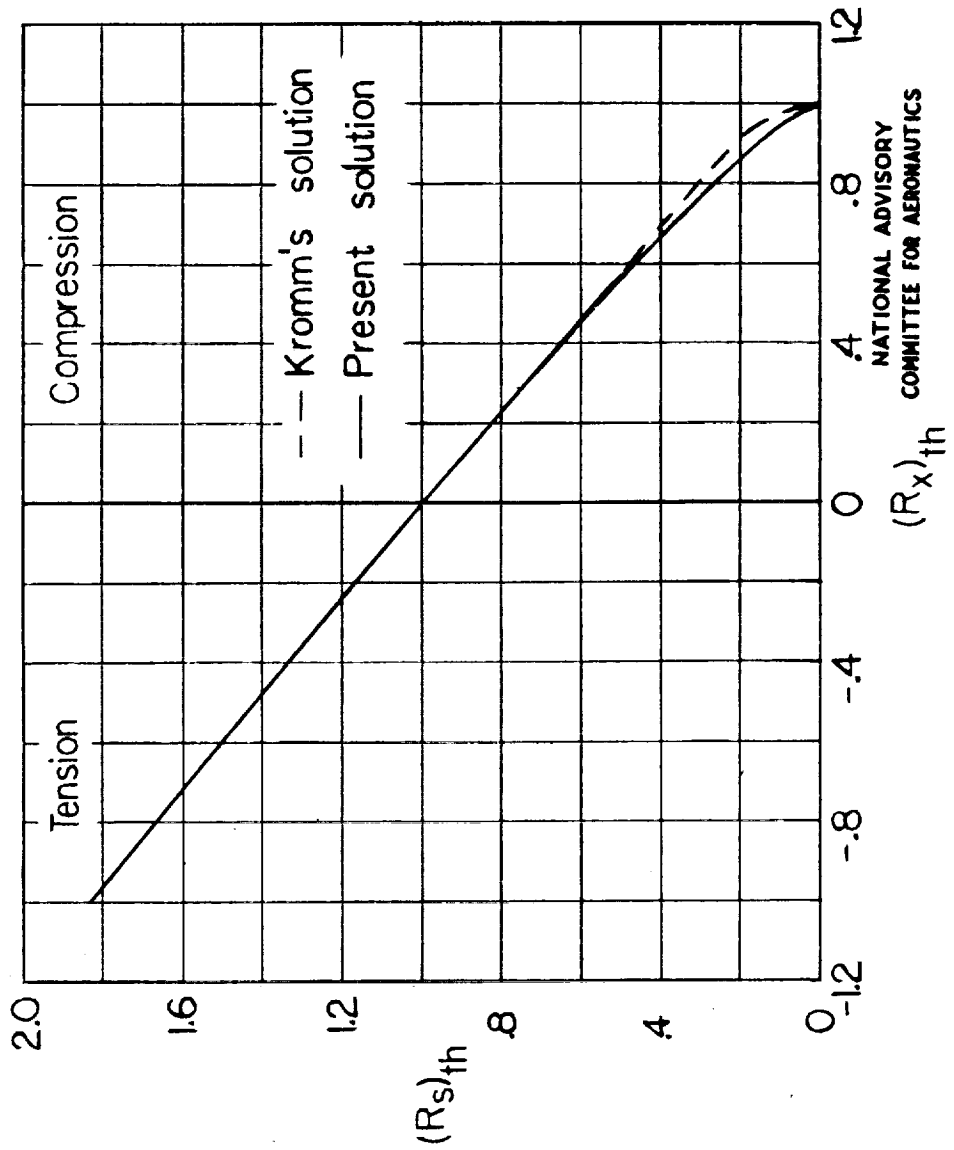


Figure 7.- Comparison of Kromm's solution with present solution for simply supported cylinders of  $Z > 100$ .

60  
65

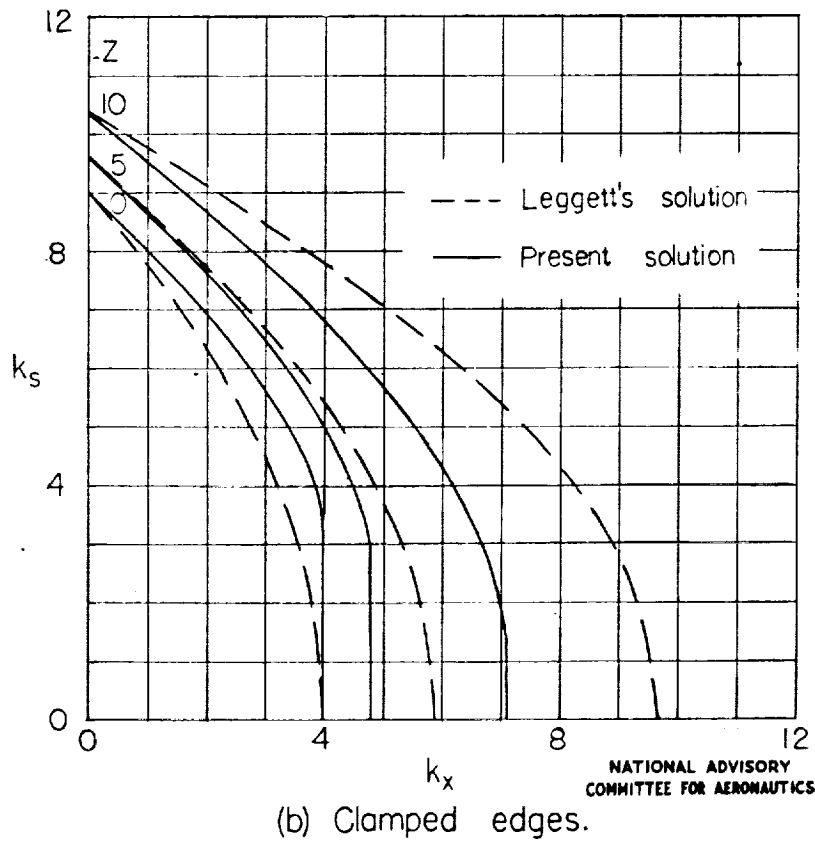
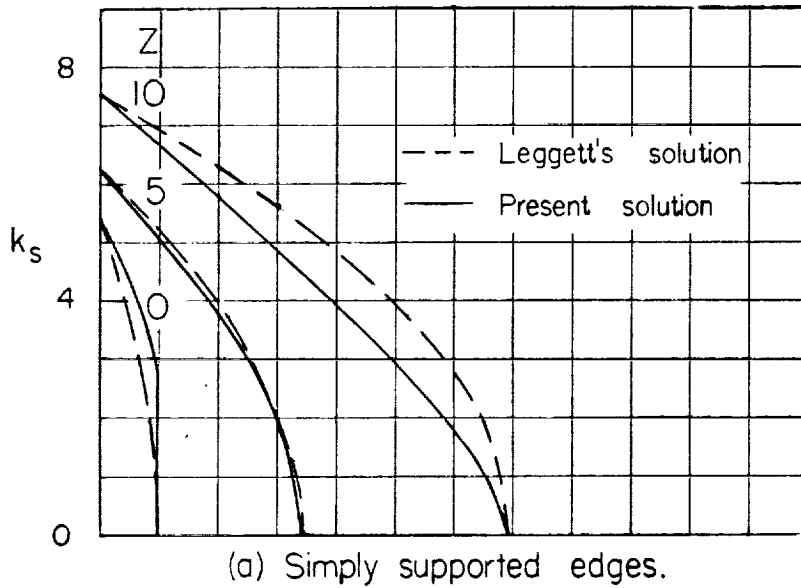


Figure 8.- Comparison of Leggett's solutions with present solutions for cylinders.